Scientific Research Publishing

Journal of Power and Energy Engineering, 2025, 13(12), 1-13
https://www.scirp.org/journal/jpee
ISSN Online: 2327-5901
ISSN Print: 2327-588X

Band Gap Energy and Photocatalytic Efficiency of TiO_2 Thin Films Deposited via Dip and Spin Coating under Visible Light

Zulkifli Mohd Rosli[1], Nur Dalilah Johari[2]

[1]Faculty of Industrial and Manufacturing Technology and Engineering, Universiti Teknikal Malaysia Melaka, Hang Tuah Jaya, Melaka, Malaysia
[2]Faculty of Mechanical Engineering, Universiti Teknologi Malaysia, Johor, Malaysia
Email: zmr@utem.edu.my

How to cite this paper: Rosli, Z.M. and Johari, N.D. (2025) Band Gap Energy and Photocatalytic Efficiency of TiO_2 Thin Films Deposited via Dip and Spin Coating under Visible Light. *Journal of Power and Energy Engineering*, **13**, 1-13.
https://doi.org/10.4236/jpee.2025.1312001

Received: November 12, 2025
Accepted: December 5, 2025
Published: December 8, 2025

Abstract

TiO_2 thin films were prepared via a water-based sol-gel method and deposited using dip and spin coating techniques to investigate the relationship between band gap energy and photocatalytic efficiency under visible light irradiation. The influence of deposition method and annealing temperature on the structural phase, optical properties, and methylene blue (MB) degradation performance was examined. Dip-coated films exhibited a transition from anatase to a mixed anatase-rutile phase above 300˚C, while spin-coated films predominantly formed the brookite phase. The band gap of dip-coated films decreased from 2.81 eV at 200˚C to 2.48 eV at 500˚C, whereas spin-coated films showed a minimum of 2.45 eV at 300˚C, achieving the highest MB degradation efficiency of 97.7%. Higher temperatures led to band gap widening and reduced photocatalytic activity. These findings demonstrate that spin-coated TiO_2 thin films annealed at 300˚C exhibit optimal structural and optical properties for visible-light-driven photocatalysis.

Keywords

TiO_2 Thin Films, Photocatalysis, Spin Coating, Methylene Blue, Sol-Gel, Dip Coating

1. Introduction

Semiconductor photocatalysts such as titanium dioxide (TiO_2) [1], cerium oxide (CeO_2) [2], and zinc oxide (ZnO) [3] have been widely investigated for the photodegradation of organic dyes due to their high photocatalytic activity. Among

them, TiO_2 has received significant attention owing to its excellent chemical stability, non-toxicity, affordability, and inertness [1]. In photocatalytic applications, thin-film photocatalysts are often preferred over powdered forms because they offer greater usability, mechanical stability, and ease of recovery [4].

Various modification strategies have been developed to enhance the photocatalytic efficiency of TiO_2 thin films, including semiconductor coupling, doping, and compositional mixing. For example, Upadhaya *et al.* [5] synthesized ZnO/TiO_2 thin films via the sol-gel spin-coating method using isopropanol and monoethanolamine as solvents, achieving 94% methylene blue (MB) degradation under UV light. Similarly, Li *et al.* [6] fabricated NiW/TiO_2 coatings using sodium citrate as a complexing agent, attaining 60.7% MB degradation. In another study, Jeong and Lee [7] prepared TiO_2-coated glass via dip coating in an ammonia solution, achieving 34% MB degradation under visible light.

Most TiO_2 thin films are synthesized using sol-gel methods, followed by deposition techniques such as dip coating and spin coating. These conventional processes often rely on organic solvents and additives, which assist in film formation and stabilization but pose toxicity and environmental hazards [8]. The presence of various organic functional groups in these solvents can lead to ecological damage when released into wastewater [9]. To mitigate these issues, researchers have increasingly adopted water-based sol-gel methods as sustainable alternatives. These green synthesis routes align with the principles of green technology by minimizing hazardous waste, improving safety, and reducing environmental impact.

In this context, TiO_2 thin films synthesized via water-based sol-gel methods offer a promising approach for sustainable photocatalytic applications. The present study involves characterization and investigation on photocatalytic properties of TiO_2 thin films prepared using dip coating and spin coating techniques. Specifically, it compares their crystalline phases, cross section morphology, band gap energies and correlates these to the coatings' photocatalytic efficiency under visible light irradiation.

2. Materials and Methods

2.1. Synthesis of TiO_2 Thin Films

Mixing 0.2 M of titanium (IV) isopropoxide precursor (TTIP, 97%, Sigma Aldrich) and 64 ml of deionized water (DI) was used to prepare TiO_2 sol. The TTIP was added drop by drop (1 drop/minute). Then, 0.4 ml of hydrochloric acid (HCl, 37%, Merck) was poured into the solution. The solution was stirred for 3 hours. After that, the solution was allowed to age for 48 hours.

The glass substrate was submerged in the TiO_2 sol using a TEFINI Model DP1000 precision single dip coater equipment. The glass substrates were submerged in the solution with a dipping withdrawal speed of 0.5 mm/second and a dwell duration of 90 seconds to ensure minimal coating deposition, as previously investigated and verified in prior project studies [10]. To finish the single dipping number, the samples were dried at room temperature for 30 minutes before being

dried in an oven at 110˚C for 30 minutes. This dipping step was repeated ten times to produce a homogeneous coating. The thin films were permitted throughout the oven to dry at 110˚C for 1 hour.

For the spin coating process, 90 µL of TiO_2 sol was dispensed onto the surface of a glass substrate using an Eppendorf pipette. The substrate was secured to a vacuum-assisted spin coater and spun at a fixed speed of 1500 rpm for 30 seconds. This process was repeated twice. The deposited TiO_2 thin films were then dried in an oven at 110˚C for 1 hour. For the final treatment, both dip-coated and spin-coated TiO_2 thin films were heat-treated at 200˚C, 300˚C, 400˚C, and 500˚C for 3 hours, with a heating rate of 5˚C/min.

2.2. Characterization of TiO_2 Thin Films

Structural of the TiO_2 thin films was performed with X-ray diffractometer (XRD) PANalytical X'PERT PRO MPD Model PW 3060/60 within the range of 10˚ - 80˚. The cross-section morphology of TiO_2 thin films was observed by scanning electron microscope (SEM) with a ZEIS EVO 50. While EDX analysis was run with JEOL model JSM-6010PLUS/LV. The optical absorption of TiO_2 thin films was measured by Lambda 35 UV-Vis spectrometer, Perkin Elmer with wavelength ranges of 200 nm - 1100 nm. The band gap of the TiO_2 thin films was calculated with the Tauc plot method.

2.3. Photocatalytic Test for TiO_2 Thin Films

The photocatalytic test was carried out using an OSRAM model with 200 Watt of visible radiation function as a light source 16 cm distant from the dye solution. The temperature in the chamber was maintained at about 25˚C using a cooling fan. A TiO_2 thin film coating was submerged in 25 ml with a concentration of 1 x 10^{-6} M methylene blue (MB) in a beaker as part of this experiment [11]. To guarantee that the adsorption-desorption equilibrium was attained to radiation, the methylene blue solution with photocatalyst (TiO_2 thin film coating) sample was maintained in the dark for 30 min. The dyes were taken and the absorbance was measured every 1 hour.

The degradation of the MB solution was measured at 665 nm and the SHIMADZU UV-1700 UV-Vis spectrometer was used to analyze the degradation of MB derived by residual absorbance. The reduction in absorbance indicates that MB is degrading. Equation 1 was used to compute the percentage of MB deterioration. The test was replicated 3 times to increase the accuracy and reliability of the results.

$$Degradation\ (\%) = \frac{C_o - C}{C_o} = \frac{A_o - A}{A_o} \qquad \text{Equation 1}$$

where C_o denotes the starting concentration after equilibrium adsorption, C denotes the MB solution's response concentration, A_o denotes the initial absorbance, and A denotes the MB solution's altered absorbance.

3. Results

3.1. Characterization of TiO_2 Thin Films

Figure 1 shows the XRD patterns of the deposited TiO_2 thin films obtained through dip and spin coating at various heat treatment temperatures. As shown in Figure 1(a), the TiO_2 thin films fabricated through dip coating consist of a mixture of anatase and rutile. The anatase and rutile were compared to the standard JCPDS No. of 21-1271 and 75-1753, respectively. The TiO_2 thin film heated at 200˚C was produced only anatase (101) at 2θ of 25˚. When heated at 300˚C, the anatase (101) and rutile (110) were recognized only at 2θ of 25˚ and 27˚, respectively. At 400˚C and 500˚C, three peaks of anatase (101), (200) and (105) were identified at 2θ of 25˚, 48˚ and 54˚ together with rutile (110) at 2θ of 27˚. The relative intensity of anatase and rutile peaks increased with increased heat treatment temperature. This higher relative intensity designated an increased degree of crystallization [12]. After heat treatment temperature was used, the crystallization process occurred during nucleation and growth procedures. In addition, the occurrence of phase transformations is influenced by the heat treatment temperature of the thermal treatment and surface defects of the materials [13].

Meanwhile, Figure 1(b) shows the XRD patterns of TiO_2 thin films fabricated through spin coating. The XRD patterns of TiO_2 thin film heated at 200˚C displayed brookite peaks (111) and (023) at 2θ of 31˚ and 66˚, respectively. The brookite peak (111) at 2θ of 31˚ with d-spacing of 2.8 Å was compared to the standard JCPDS No. of 84-1750 that had a standard of $2\theta = 31.3$˚ with d-spacing of 2.81 Å and different with the standard JCPDS No. 29-1360 ($2\theta = 30.8$˚, d-spacing of 2.9 Å). At 300˚C and 400˚C, the XRD patterns showed only a single brookite peak (111) produced at 2θ of 31˚. As can be seen from the figure, the relative intensity of the brookite (111) showed a decrease with increased heat treatment temperature. Once the heat treatment temperature was raised to 500˚C, the XRD pattern became amorphous, indicating that no TiO_2 crystalline phase formed. The absence of brookite production at high temperatures of 500˚C may be due to its thermodynamically metastable nature, which prefers to exist at low temperatures [11]. Haggerty *et al.* [14] stated that designing a synthetic approach to a metastable phase of brookite necessitates an understanding of both equilibrium and non-equilibrium processes that may occur. Although phase diagrams of the bulk Ti-O system under standard conditions have been developed, phase selection during synthesis is not just an issue of bulk equilibrium thermodynamics, as indicated by the prevalence of metastable, non-equilibrium synthesis products such as brookite. As previously observed in comparable ionic systems, synthesis routes to various stable and metastable phases can be influenced by finite-size effects, nucleation kinetics, bulk and surface off-stoichiometry.

This is also consistent with the findings of Allen *et al.* [15] who found that at 110˚C, 39.7% of the brookite crystalline phase had dropped to 15.1% when the temperature was raised to 600˚C. Furthermore, at temperatures of 700˚C and higher, brookite is not detected. It seems to be possible that the absence of the

TiO_2 crystalline phase is related to the lack of a solvent in the sol formulation. In the sol-gel procedure, the solvent slows the rate of hydrolysis and condensation. Thus, during the TiO_2 sol preparation, the precursor of TTIP was added at 1 drop per minute to control the hydrolysis process [10]. In addition, the use of HCl as a catalyst also controls the TiO_2 hydrolysis and nucleation rates. Herman *et al.* [16] observed that the desorption temperature for water is lower (−23.15˚C) compared to methanol (336.85˚C). As a result, it is predicted that in this study, where no solvent was employed compared to the previous study that used a common TiO_2 sol formulation, a faster rate of hydration would be seen, particularly at high temperatures, preventing crystallization at 500˚C.

The XRD results reveal that TiO_2 phase development is influenced by deposition methods. Dip coating produces a mixture of anatase and rutile, consistent with Yazid *et al.* [17] and Bakri *et al.* [12] while spin coating predominantly forms brookite, aligning with Komaraiah *et al.* [18] and Singh *et al.* [19]. The deposition method affects crystallization: spin coating promotes brookite growth through uniform seed layers, while dip coating relies on gravitational forces. WAXS analysis confirmed TiO_2 crystalline phases, unlike SAXS. These findings highlight the critical role of deposition techniques in tailoring TiO_2 thin film structures for targeted applications. Overall, the XRD analysis confirms that the TiO_2 phase formation is strongly influenced by the deposition method, with dip coating producing a mixed anatase-rutile structure, while spin coating predominantly forms brookite.

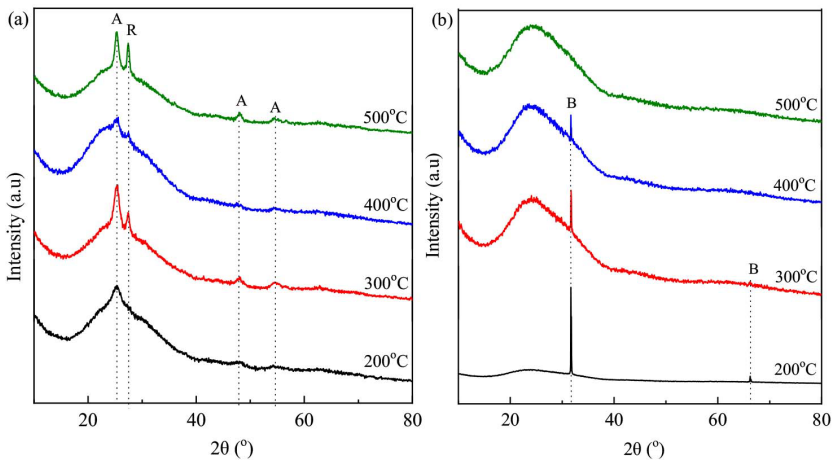

Figure 1. XRD patterns of the deposited TiO_2 thin films obtained through (a) dip and (b) spin coating at various heat treatment temperatures.

Figure 2 shows the cross-sectional morphology of the TiO_2 thin films deposited via dip and spin coating at various heat treatment temperatures. From the cross-sectional morphology of the TiO_2 thin films, the coating thickness can be determined. The cross-sectional morphology for the TiO_2 thin film deposited via dip coating shows that the thickness coating at 200˚C was 1005.9 nm. The thickness of the TiO_2 thin film deposited via dip coating decreased to 745.9 nm and 320.5

nm at 300˚C and 400˚C, respectively. However, when the heat treatment temperature was increased to 500˚C, the coating thickness of the TiO_2 thin film deposited via dip coating was increased to 679.2 nm. This is due to the agglomerate particle that can be observed from the surface morphology of the thin film.

Meanwhile, for spin coating, the cross-sectional morphology of the TiO_2 thin film at 200˚C shows that the coating thickness was 512.9 nm. When increased the heat treatment temperature to 300˚C, the coating thickness of the TiO_2 thin film was 618.7 nm. The thickness of the TiO_2 thin film deposited via spin coating at 400˚C and 500˚C was 436.6 nm and 350.6 nm, respectively. An increase in heat treatment temperature shows a decrease in the coating thickness of the TiO_2 thin film deposited via spin coating. The increase and vice versa of the coating thickness of the TiO_2 thin film is possible due to the pore size increasing as the heat treatment temperature increases [20]. The water permeance of thin films increases at first with increasing heat treatment temperature and then drops at a heat treatment temperature turning point.

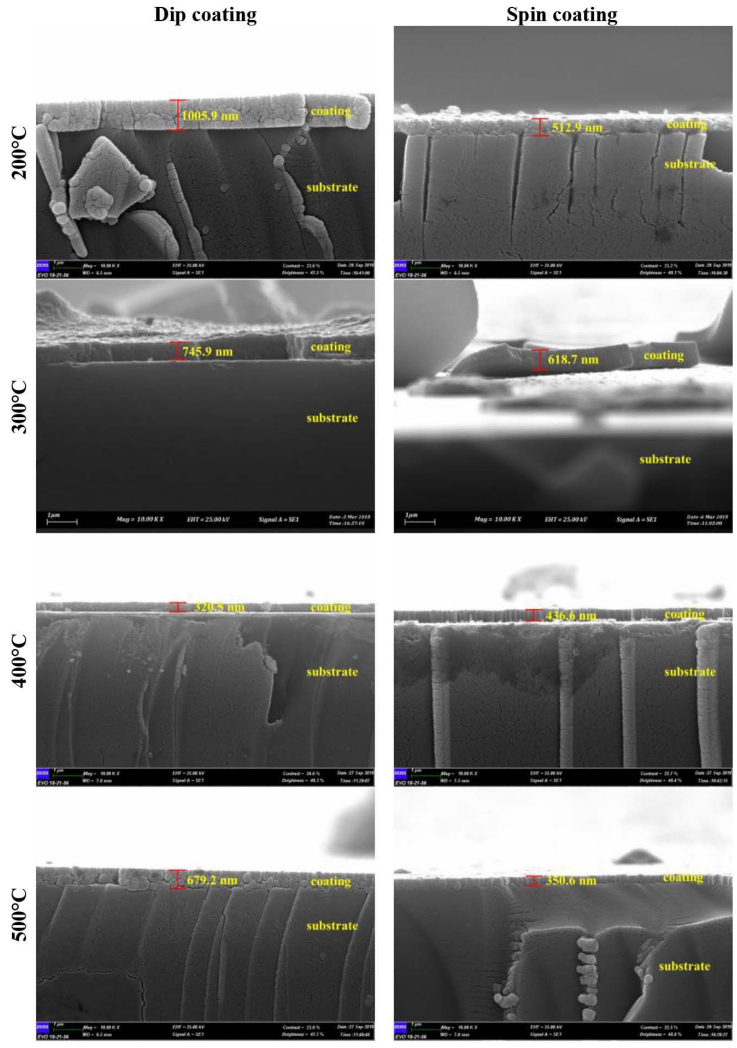

Figure 2. Cross-sectional view of the TiO_2 thin films.

Figure 3 shows FTIR spectra of TiO_2 thin film deposited via dip and spin coating heated at various heat treatment temperatures. For the dip coating (Figure 3(a)), a mixture of anatase and rutile film had the transmittance bands around 400 cm^{-1} - 800 cm^{-1} denoted to the Ti-O and/or Ti-O-Ti bonds regardless of any heat treatment temperature [21]. The transmittance band at 1532 cm^{-1} - 1693 cm^{-1} shows that the anatase and rutile film was assigned to the O-H bending mode when heated at 200˚C, 300˚C and 400˚C. Increased heat treatment temperature at 500˚C shows there is no peak at 1532 cm^{-1} - 1693 cm^{-1} and indicates that the O-H bending mode was completely removed from the film. Sadek *et al.* [21] also observed the intensity of the peak-related water absorptions decreased by increasing the annealing temperature. This is due to the elimination of O-H during the heating process, possibly by hydrogen diffusion out of crystal and oxidation of Ti3+ to Ti4+, proceed concomitantly. The FTIR spectra also show the transmittance band in the range of 2500 cm^{-1} - 3746 cm^{-1} of diluted titanium tetraisopropoxide (TTIP) in an aqueous solution due to Ti-OH and –OH vibrations [22]. This indicated the stretching vibration of the surface hydroxyl group or adsorbed water on the surface of TiO_2 samples [23].

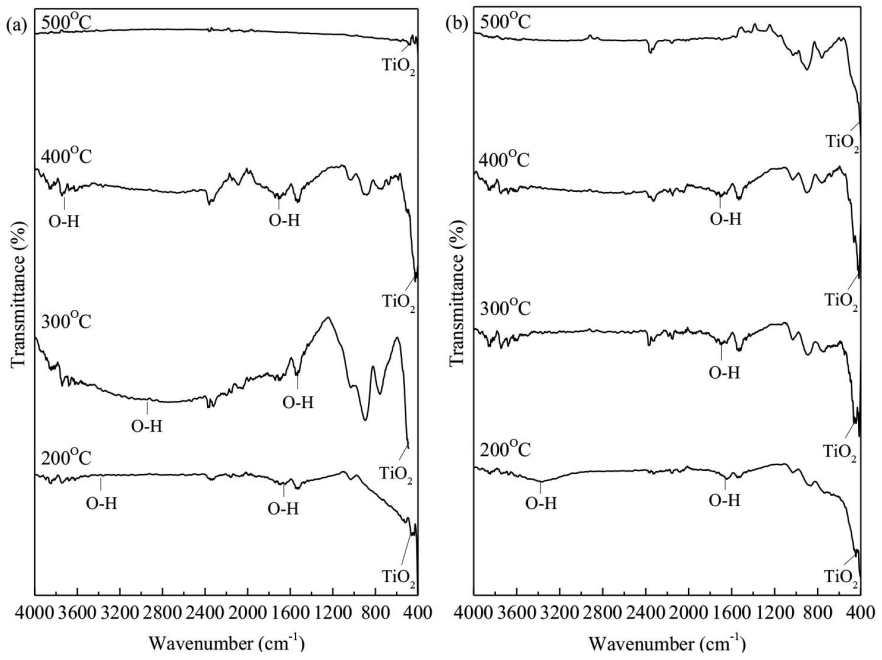

Figure 3. FTIR spectra of TiO_2 thin films deposited via (a) dip and (b) spin coating heated at various heat treatment temperatures.

While for the spin coating (Figure 3(b)), the transmittance band also existed at 400 cm^{-1} - 800 cm^{-1} was credited to Ti-O and/or Ti-O-Ti bonds regardless of deposition method and heat treatment temperature. The transmittance band at 1532 cm^{-1} - 1693 cm^{-1} at brookite film at 200˚C, 300˚C, and 400˚C were allocated to an O-H bending mode. At 500˚C, no transmittance band at 1532 cm^{-1} - 1693 cm^{-1}, and it shows the O-H bending mode was removed from the brookite film during

heating. The FTIR spectra also show the transmittance band in the range of 2500 cm^{-1} - 3746 cm^{-1} for brookite film at 200˚C where it is indicated that the dilution of TTIP in aqueous solution was due to Ti-OH and –OH vibrations. The transmittance band of 2500 cm^{-1} - 3746 cm^{-1} shows that the stretching vibration of the surface hydroxyl group or adsorbed water on the surface of brookite thin film coating [23].

In summary, the FTIR spectra show the TiO_2 thin film obtained via dip and spin coating contained the hydroxyl group on the surface of the thin film. The hydroxyl group on semiconductor surfaces is important in photocatalytic applications because it may collect photoinduced holes off the surface of materials, preventing electron-hole recombination and generating hydroxyl radicals with a high oxidation potential.

Figure 4 shows the band gap energy of the TiO_2 thin film deposited via dip and spin coating heated at various heat treatment temperatures. The band gap energy of dip-coated TiO_2 thin films varies with heat treatment temperature due to changes in crystallite size, phase composition, and structural defects. At 200˚C, the band gap energy is 2.81 eV, decreasing to 2.61 eV at 300˚C due to improved crystallinity and the formation of rutile phase, which has a lower band gap than anatase. However, at 400˚C, the band gap increases to 2.77 eV, likely due to continued anatase-to-rutile transformation, which modifies the electronic structure. At 500˚C, the band gap drops significantly to 2.48 eV, as rutile becomes the dominant phase and crystallite growth enhances charge transport. This trend indicates that heat treatment plays a crucial role in tailoring TiO_2 optical properties, making dip-coated films at 500˚C more suitable for visible-light-driven photocatalysis due to their lower band gap energy.

Meanwhile, TiO_2 thin film via spin coating has a band gap energy of 2.72 eV at 200˚C. The band gap energy of brookite thin film coating heated at 300˚C was 2.45 eV. Next, at 400˚C, the band gap energy was calculated at 3.04 eV. When the heat treatment temperature is raised to 500˚C, the band gap energy of the brookite thin film coating is 3.62 eV. The band gap energy for the brookite thin film coatings heated at 200˚C, 300˚C and 400˚C was shown in agreement with the literature [24]. From the figure, it can be observed that the band gap energy decreased when the heat treatment temperature increased from 200˚C to 300˚C.

However, the band gap energy becomes increased when the heat treatment temperature increases from 400˚C to 500˚C. Shi *et al.* [25] stated that the band gap energy was affected by the thickness coating. Shi *et al.* also reported that increasing the TiO_2 film thickness from 2.55 nm to 20.61 nm affected the optical band gap decreased from 3.718 eV to 3.417 eV. The thickness of the brookite thin film coating heated at 200˚C was 512.9 nm and at 300˚C was 618.7 nm. This thickness of the brookite thin film coating was increased affecting the decreased of the band gap energy to 2.72 eV at 200˚C and 2.45 eV at 300˚C. Yet, brookite thin film coating heated at 400˚C and 500˚C shows a decrease in the thickness measurement which is 436.6 nm and 350.6 nm, respectively. Resulting to the band gap energy

of brookite thin film coatings was 3.3.04 eV at 400˚C and 3.62 eV at 500˚C. In summary, the thickness of the film causes a shift in the optical absorbance edge and therefore a change in the band structure of the film.

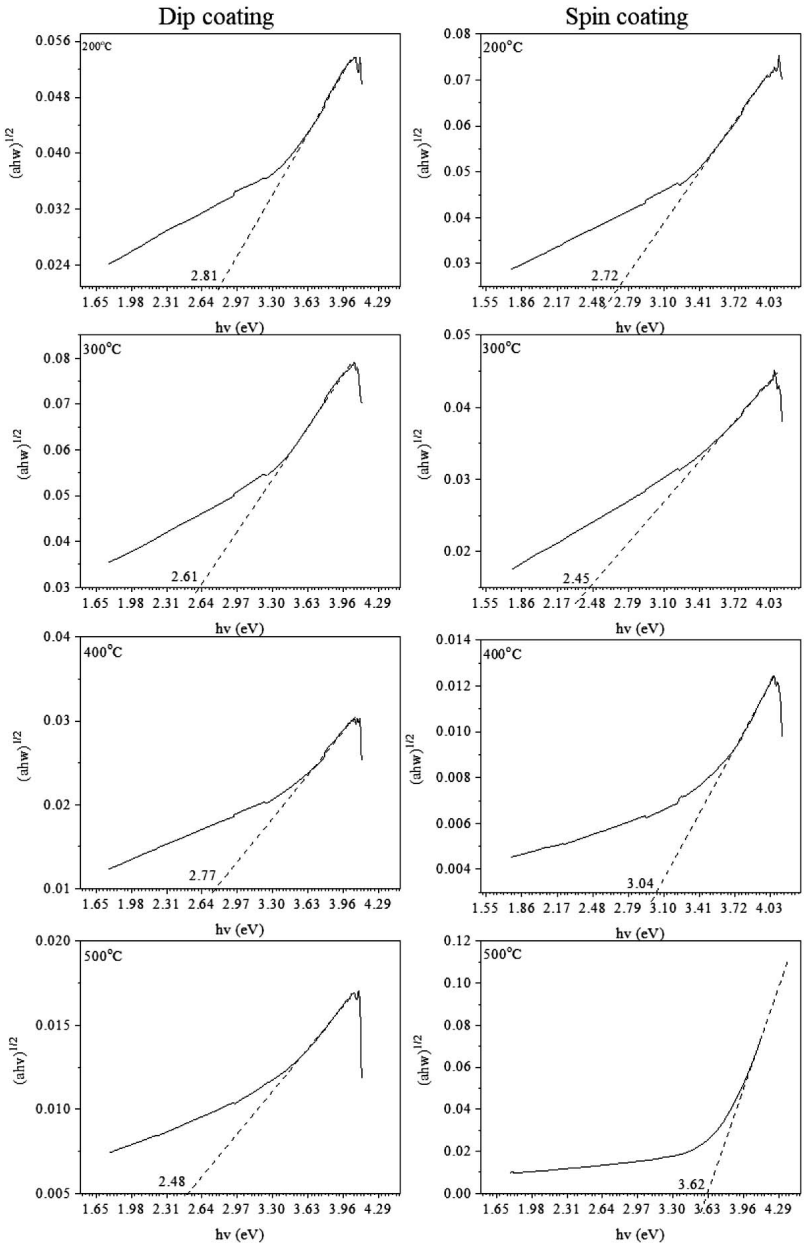

Figure 4. Band gap energy of the TiO_2 thin films at different heat treatment temperatures.

3.2. Photocatalytic Performance

Figure 5 shows the degradation efficiency of methylene blue (MB) degradation under visible light for TiO_2 thin films via dip coating and spin coating. The degradation of MB of dip-coated TiO_2 thin film shows an increase with time. Dip-coated TiO_2 thin films exhibit moderate MB degradation efficiency, primarily due to the presence of mixed anatase and rutile phases. At 200˚C, the TiO_2 thin film

showed the lowest MB degradation efficiency, achieving 72.7 ± 1.81% after 4 hours. As the heat treatment temperature increased to 300˚C, 400˚C, and 500˚C, the MB degradation efficiency also increased to 83.6 ± 2.09%, 84.5 ± 2.11%, and 84.8 ± 2.12%, respectively. The anatase phase is known for its high photocatalytic activity, while rutile has a narrower band gap, allowing for better light absorption in the visible spectrum. The low MB degradation at 200˚C is attributed to the larger band gap energy, whereas at 500˚C, the band gap energy decreased to 2.48 eV, enhancing photocatalytic activity.

For spin coating, the highest MB degradation efficiency was observed in the TiO_2 thin film heated at 300˚C, achieving 97.7 ± 2.44% after 4 hours, followed by the film heated at 200˚C, which achieved 95.3 ± 2.38%. However, as the heat treatment temperature increased to 400˚C and 500˚C, the MB degradation efficiency decreased significantly to 53.0 ± 1.32% and 51.8 ± 1.29%, respectively. A similar factor contributing to the high MB degradation efficiency at 300˚C was its lower band gap energy (2.45 eV) compared to other temperatures.

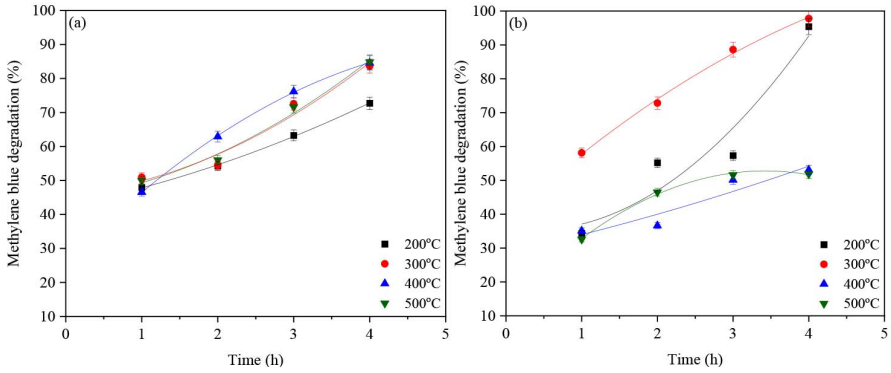

Figure 5. Degradation efficiency of methylene blue degradation under visible light for TiO_2 thin films via (a) dip coating and (b) spin coating.

4. Discussion

The photocatalytic degradation of methylene blue (MB) using TiO_2 thin films was influenced by phase composition, surface morphology, band gap energy, and heat treatment temperature. The deposition method played a crucial role in determining these properties, with dip-coated films forming a mixed anatase-rutile structure and spin-coated films predominantly exhibiting the brookite phase. XRD studies revealed that dip-coated films shifted from pure anatase to an agitated anatase-rutile mixture much above 300˚C; therefore, photodegradability [26]. However, these films were not disintegrated at temperatures up to 300˚C, where brookite remained stable. Meanwhile, higher temperatures destabilized brookite, allowing the formation of amorphous TiO_2 that later on contributed to better charge transport that led to grain growth. Therefore, the overall crystallite size increased with increase in high temperature and consequently reduced the active surface area as shown in the increase of coating thickness.

Optical band gap energy followed heat treatment for TiO_2 films. For dip-coated,

the band gap decreased from 2.81 eV at 200˚C to 2.48 eV at 500˚C because of increasing rutile, which makes it have a higher visible light absorption [27]. Meanwhile, spin-coated films had the least band gap energy at 300˚C (2.45 eV), with this temperature corresponding to the best MB degradation efficiency recorded at 97.7%. Increasing the temperature made the band gap widen, limiting the absorption of visible light and thus photocatalytic activity.

These results of MB degradation substantiate that spin-coated TiO_2 thin films at 300˚C have the best photocatalytic efficiency attributed to their brookite phase, low band gap, and uniform morphology. Dip-coated films were moderately effective but were limited by increased cracking and band gaps at higher temperature treatments. The findings demonstrate that the techniques and conditions applied in thermal treatment and deposition largely improve TiO_2 photocatalyst for wastewater remediation.

Acknowledgements

The authors would like to acknowledge the Faculty of Industrial and Manufacturing Technology and Engineering, Universiti Teknikal Malaysia Melaka (UTeM) for the support of this research and dissemination of findings.

Conflicts of Interest

The authors declare no conflicts of interest regarding the publication of this paper.

References

[1] Meena, H.M., Kukreti, S. and Jassal, P.S. (2025) Synthesis of a Novel Chitosan-TiO_2 Nanocomposite as an Efficient Adsorbent for the Removal of Methylene Blue Cationic Dye from Wastewater. *Journal of Molecular Structure*, **1319**, Article 139420. https://doi.org/10.1016/j.molstruc.2024.139420

[2] Ghamarpoor, R., Fallah, A., Jamshidi, M. and Salehfekr, S. (2023) Using Waste Silver Metal in Synthesis of Z-Scheme Ag@WO_3-CeO_2 Heterojunction to Increase Photodegradation and Electrochemical Performances. *Journal of Industrial and Engineering Chemistry*, **128**, 459-471. https://doi.org/10.1016/j.jiec.2023.08.010

[3] Eftekharipour, F., Jamshidi, M. and Ghamarpoor, R. (2023) Fabricating Core-Shell of Silane Modified Nano ZnO; Effects on Photocatalytic Degradation of Benzene in Air Using Acrylic Nanocomposite. *Alexandria Engineering Journal*, **70**, 273-288. https://doi.org/10.1016/j.aej.2023.02.047

[4] Khalifa, Z.S., Shaban, M. and Ahmed, I.A. (2023) Photocatalytic Degradation of Methyl Orange and Methylene Blue Dyes by Engineering the Surface Nano-Textures of TiO_2 Thin Films Deposited at Different Temperatures via MOCVD. *Molecules*, **28**, Article 1160. https://doi.org/10.3390/molecules28031160

[5] Upadhaya, D., Kumar, P. and Dhar Purkayastha, D. (2019) Superhydrophobic ZnO/TiO_2 Heterostructure with Significantly Enhanced Photocatalytic Activity. *Journal of Materials Science: Materials in Electronics*, **30**, 10399-10407. https://doi.org/10.1007/s10854-019-01381-2

[6] Li, S., Xianzhen, Z., Qihua, J., Zhongming, Z. and Huabo, Z. (2024) Study on the Corrosion Resistance of Electrodeposited NiW/TiO_2 Composite Coating and Its Ap-

plication in Methylene Blue Degradation in Simulated Wastewater. *International Journal of Electrochemical Science*, **19**, Article 100875. https://doi.org/10.1016/j.ijoes.2024.100875

[7] Jeong, J.E. and Lee, C. (2024) Structural Properties and Photocatalytic Activity of Amorphous-Crystalline TiO_2 Thin Films. *Thin Solid Films*, **788**, Article 140178. https://doi.org/10.1016/j.tsf.2023.140178

[8] Bakar, N.H.A., Yusop, H.M., Ismail, W.N.W., *et al.* (2022) Sol-Gel Finishing for Protective Fabrics. *Biointerface Research in Applied Chemistry*, **13**, Article 283.

[9] Raja Sekharan, T., Margret Chandira, R., Tamilvana, S., *et al.* (2022) Deep Eutectic Solvents as an Alternate to Other Harmful Solvents. *Biointerface Research in Applied Chemistry*, **12**, 847-860.

[10] Johari, N.D., Rosli, Z.M., Juoi, J.M. and Yazid, S.A. (2019) Comparison on the TiO_2 Crystalline Phases Deposited via Dip and Spin Coating Using Green Sol-Gel Route. *Journal of Materials Research and Technology*, **8**, 2350-2358. https://doi.org/10.1016/j.jmrt.2019.04.018

[11] Johari, N.D., Rosli, Z.M. and Juoi, J.M. (2022) Effect of Heat Treatment Temperature on the Structural, Morphological, Optical and Water Contact Angle Properties of Brookite TiO_2 Thin Film Deposited via Green Sol-Gel Route for Photocatalytic Activity. *Journal of Materials Science*: *Materials in Electronics*, **33**, 15143-15155. https://doi.org/10.1007/s10854-022-08433-0

[12] Bakri, A.S., Sahdan, M.Z., Adriyanto, F., Raship, N.A., Said, N.D.M., Abdullah, S.A., *et al.* (2017) Effect of Annealing Temperature of Titanium Dioxide Thin Films on Structural and Electrical Properties. *AIP Conference Proceedings*, **1788**, Article 030030. https://doi.org/10.1063/1.4968283

[13] Catauro, M., Tranquillo, E., Dal Poggetto, G., Pasquali, M., Dell'Era, A. and Vecchio Ciprioti, S. (2018) Influence of the Heat Treatment on the Particles Size and on the Crystalline Phase of TiO_2 Synthesized by the Sol-Gel Method. *Materials*, **11**, Article 2364. https://doi.org/10.3390/ma11122364

[14] Haggerty, J.E.S., Schelhas, L.T., Kitchaev, D.A., Mangum, J.S., Garten, L.M., Sun, W., *et al.* (2017) High-Fraction Brookite Films from Amorphous Precursors. *Scientific Reports*, **7**, Article No. 15232. https://doi.org/10.1038/s41598-017-15364-y

[15] Allen, N.S., Mahdjoub, N., Vishnyakov, V., Kelly, P.J. and Kriek, R.J. (2018) The Effect of Crystalline Phase (Anatase, Brookite and Rutile) and Size on the Photocatalytic Activity of Calcined Polymorphic Titanium Dioxide (TiO_2). *Polymer Degradation and Stability*, **150**, 31-36. https://doi.org/10.1016/j.polymdegradstab.2018.02.008

[16] Herman, G.S., Dohnálek, Z., Ruzycki, N. and Diebold, U. (2003) Experimental Investigation of the Interaction of Water and Methanol with Anatase-TiO_2(101). *The Journal of Physical Chemistry B*, **107**, 2788-2795. https://doi.org/10.1021/jp0275544

[17] Yazid, S.A., Rosli, Z.M. and Juoi, J.M. (2019) Effect of Titanium (IV) Isopropoxide Molarity on the Crystallinity and Photocatalytic Activity of Titanium Dioxide Thin Film Deposited via Green Sol-Gel Route. *Journal of Materials Research and Technology*, **8**, 1434-1439. https://doi.org/10.1016/j.jmrt.2018.10.009

[18] Komaraiah, D., P.Madhukar,, Vijayakumar, Y., Ramana Reddy, M.V. and Sayanna, R. (2016) Photocatalytic Degradation Study of Methylene Blue by Brookite TiO_2 Thin Film under Visible Light Irradiation. *Materials Today*: *Proceedings*, **3**, 3770-3778. https://doi.org/10.1016/j.matpr.2016.11.026

[19] Singh, M., Duklan, N., Singh, P. and Sharma, J. (2018) Synthesis and Photocatalytic Activity of Anatase TiO_2 Nanoparticles for Degradation of Methyl Orange. *AIP Conference Proceedings*, **1953**, Article 030075. https://doi.org/10.1063/1.5032410

[20] Ghouil, B., Harabi, A., Bouzerara, F., Boudaira, B., Guechi, A., Demir, M.M., *et al.* (2015) Development and Characterization of Tubular Composite Ceramic Membranes Using Natural Alumino-Silicates for Microfiltration Applications. *Materials Characterization*, **103**, 18-27. https://doi.org/10.1016/j.matchar.2015.03.009

[21] Sadek, O., Touhtouh, S., Rkhis, M. and Hajjaji, A. (2024) Study of the Hydroxylation of the TiO_2 Thin Layer Prepared by Spin-Coating Method Using FTIR Analysis and DFT Theory. *Inorganic Chemistry Communications*, **161**, Article 112092. https://doi.org/10.1016/j.inoche.2024.112092

[22] Lim, D., Kim, S., Kong, H., Nam, D., Shim, S.E. and Baeck, S. (2018) Facile Analytical Methods to Determine the Purity of Titanium Tetrachloride. *International Journal of Analytical Chemistry*, **2018**, 1-5. https://doi.org/10.1155/2018/6470196

[23] Jnido, G., Ohms, G. and Viöl, W. (2019) Deposition of TiO_2 Thin Films on Wood Substrate by an Air Atmospheric Pressure Plasma Jet. *Coatings*, **9**, Article 441. https://doi.org/10.3390/coatings9070441

[24] Monai, M., Montini, T. and Fornasiero, P. (2017) Brookite: Nothing New under the Sun? *Catalysts*, **7**, Article 304. https://doi.org/10.3390/catal7100304

[25] Shi, Y.J., Zhang, R.J., Zheng, H., Li, D.H., *et al.* (2017) Optical Constants and Band Gap Evolution with Phase Transition in Sub-20-nm-Thick TiO_2 Films Prepared by ALD. *Nanoscale Research Letters*, **12**, Article No. 243. https://doi.org/10.1186/s11671-017-2011-2

[26] Bagheri, S. and Julkapli, N.M. (2017) Mixed-Phase TiO_2 Photocatalysis: Correlation between Phase Composition and Photodecomposition of Water Pollutants. *Reviews in Inorganic Chemistry*, **37**, 11-28. https://doi.org/10.1515/revic-2016-0001

[27] Arora, I., Chawla, H., Chandra, A., Sagadevan, S. and Garg, S. (2022) Advances in the Strategies for Enhancing the Photocatalytic Activity of TiO_2: Conversion from UV-Light Active to Visible-Light Active Photocatalyst. *Inorganic Chemistry Communications*, **143**, Article 109700. https://doi.org/10.1016/j.inoche.2022.109700